

# Spatially-fed arrays for near-field multiple-spot coverage

Álvaro Fernández Vaquero, Manuel Arrebola, Marcos R Pino

Group of Signal Theory and Communications, Universidad de Oviedo, Gijón, Spain

{fernandezvalvaro, arrebola, mpino}@uniovi.es

**Abstract**—A transmitarray antenna working at 28 GHz is proposed as a base station for novel indoor communications, including 5-G, Internet of Things (IoT) and wireless power transfer. This antenna produces a near-field coverage area in a desire area wherein the device should be found, giving them a total connectivity with external but also internal networks. Concerning the feeder, instead of using a single feeder configuration a cluster of them is selected. This cluster works in the 28 GHz band but using different channel which improves the capacity of the base station. In addition, a Phase-Only Synthesis (POS) is carried out in order to improve the features of the near-field coverage but only for the central feed and the final performances are evaluated for all the spots.

**Index Terms**—Transmitarray, 5-G, indoor communications, near-field, generalized Intersection Approach

## I. INTRODUCTION

The advent of 5G technology has sparked a constant need in the evolution of the communications systems, since new challenges have arrived. Particularly, wireless communications are a current topic where the new systems have to lead with high data rates or being as fast and sophisticated as possible. Conversely, there is another big challenge regarding the users, 5G involves to increase the capacity of these communications in order to support a massive number of users, wherein not only phone users are presented, but also there will be a myriad of other devices such as sensors or electronic appliances. All of the elements belonging to 5G will demand the best performance in terms of bandwidth, data rates or efficiency, so chosen a proper frequency to develop wireless communications is a critical point. In this line, the sub-6 set gathers all the frequencies lower than 6 GHz and then, the millimetre-wave mainly focuses on 28, 39 and 60 GHz which is considered as an excellent opportunity for this new generation. Another important point is the location of the devices, which are highly likely to be placed at an unique position and, generally, in an indoor scenario. Therefore, this range of frequencies are particularly good for developing efficient indoor communications, allowing to reach all the features mentioned. Summarizing, one of the biggest goals of 5G is reaching a total connectivity among devices, good performances and distinguished to indoor communications.

This work was supported in part by the Ministerio de Ciencia, Innovación y Universidades under project TEC2017-86619-R (ARTEINE) and by the Gobierno del Principado de Asturias/FEDER under Project GRUPIN-IDI/2018/000191

Foregoing points leads to define specific areas with lot of devices that require connectivity, not only with external networks but also among them. Thus, this new scenario implies forgetting extensive coverage areas in support of little areas mainly focuses on the areas wherein the devices are placed or, in other words, developing personal indoor coverage areas or femtocells. Although this idea is apparently against massive MIMO, which seems to be one of the best solutions for 5G communications [1] [2], the complexity of the scenario in indoor communications requires to find a less complex solution. In this case, femtocells are potentially more interesting for this kind of communications.

Bearing in mind that the femtocell has a small size just for the devices that are placed on a specific area and, the working frequency is within the millimetre-wave spectrum, the best idea regarding the base station, seems to place it in a position close to the devices. This mainly leads to work in the near-field region of the base station and locate the structure in the same spot of the devices. Therefore, relying the spot, it could be highly important to provide base stations with a really compact structure in order to ensure a high mimetization with the surroundings, as it can happens in a working area such as offices [3]. Concerning the radiated power by the station, the concentration of this power in the desire area, avoiding any other directions, helps to improve the efficiency of the base station. Because of these points, spatially-fed arrays such as reflectarrays or transmitarrays can be considered as potential candidates to use them in the antenna of the base station. Both are low-profile antenna that can reach a very compact structure making feasible their integration in the indoor scenario. Then, there are several works in which both far and near-field are synthesis for improving the performance of this antennas in communications [4], [5]. For instance, in [6] the near-field of a reflectarray was optimized to create a large flat area in a working area.

In this work, a transmitarray is proposed since the chance of using a central configuration can provide a more compact structure, avoiding the block losses or having an offset plane in the radiated field due to the feed location. Additionally, there is another important novelty regarding the feed, which is based on the use of a cluster instead of a single one, as happens in [6]. This cluster works at the same frequency but different channels so, the capacity of the base station is increased. Concerning the near-field coverage area, the use of different feeds generates as many spots as the number of the

cluster elements. Then, in order to improve the performances of these spots a near-field optimization is required, which is performed using the generalized Intersection Approach (IA) algorithm. It should be underlined that this optimization is only done for one feed, notwithstanding the other feeds are also improved due to the properties of the transmitarray. In addition, this technique helps to decrease the complexity of a multi-spot coverage optimization.

## II. SPATIALLY-FED ARRAY FOR MULTIPLE-SPOT COVERAGE

A transmitarray fed by a cluster of feeds is used to generate multiples beams in different directions, making a multiple-spot coverage area. Initially, the transmitarray is properly designed for a central feed, which radiates a beam in a certain direction and generates an unique spot area. Thus, the position of the cluster is defined to ensure a good behaviour for all the feeds.

According to the working principle of a transmitarray, if a feed is located in a position where the amplitude of the incident field is similar to the amplitude of the incident field provided by the central feed, the transmitted field will be very similar in amplitude but not in phase. The phase of the transmitted field will be the sum of two components: the phase of the incident field produced by each feed and different for each one, and the phase-shift introduced by the cells of the transmitarray. Usually the cell of a transmitarray antenna is designed to ensure angular stability which means that the phase-shift is not much sensible with the angle of the impinging wave. In this case, the major change in the phase of the transmitted field will be produced by the different illumination of each feed. Taking Fig. 1 as reference, the feeds have to be placed in the arc defined by the midpoint of each transmitarray edge and the central feed, ensuring the same distance from the feed to the centre of the lens for the whole cluster.

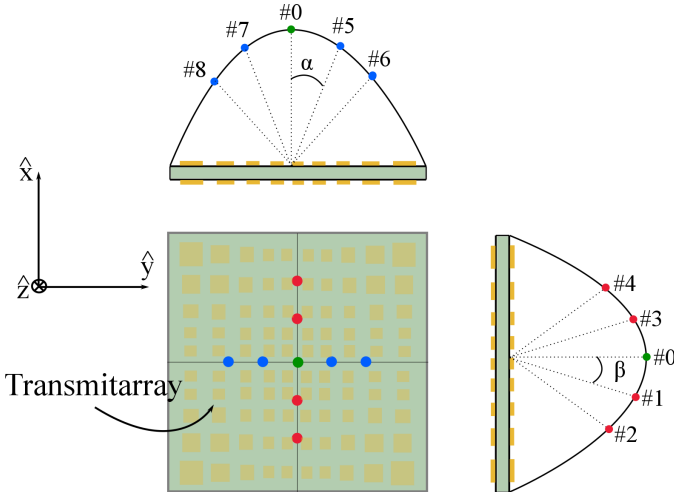


Fig. 1: Distribution of the different feeds.

The scenario used in this work is a cluster of 9 feeds, where each feed is separated an angular distance of  $10^\circ$ , which are defined by the angle  $\beta$  for the  $xz$  cut and  $\alpha$  for the  $yz$

cut (see Fig.1). Then, the transmitarray and the cluster are located close to the ceiling and over a table where are placed the devices that require any kind of connectivity. Regarding the near-field radiated by this setup, Fig. 2 shows how the angular separation of the feeds is also the spatial separation of the beams. Therefore, using the 9 feeds it is feasible to generate the same number of beams with an angular range of  $20^\circ$ . As Fig. 2 shows, the goal is to generate 9 different spot coverage area with reduced overlapping in order to work as a single coverage area. The position of spot area can be controlled by just changing the angles  $\beta$  and  $\alpha$ , but the size of the spot requires to carry out a near-field spot synthesis. In this case, the near-field synthesis tool is based on the generalized Intersection Approach algorithm. The goal of the synthesis process is to reach a near-field multi-spot coverage area as the one despices in Fig. 3, where the contour of the minimum area with less than 1 dB of amplitude ripple is shown for each beam. Using the coordinate reference system defined in Fig. 2 as reference, this specification is defined in a  $z$ -constant plane at  $z = 1.8$  m, which is within the near-field region and corresponds to the desktop surface.

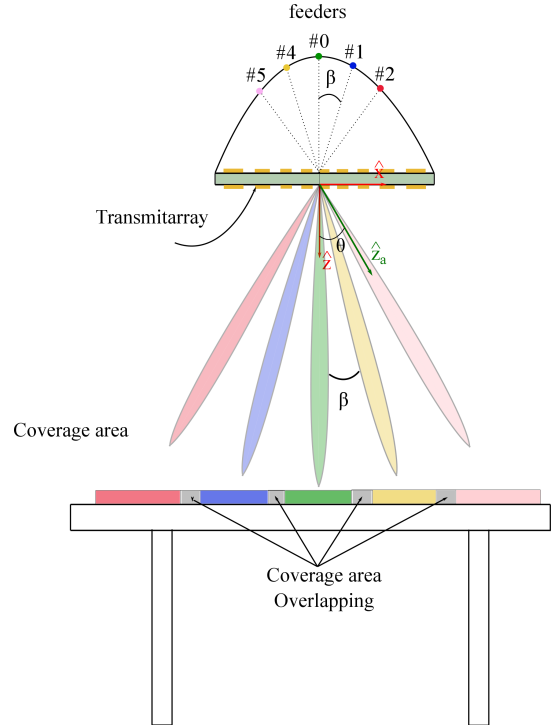


Fig. 2: Distribution of the different beams.

## III. GENERALIZED INTESECTION APPROACH FOR NEAR-FIELD PHASE-ONLY SYNTHESIS

The generalized Intersection Approach is chosen to carried out a phase-only synthesis (POS) of the near-fiel radiated by the transmitarray. Most of the optimization algorithms try to minimize a cost function, nevertheless, the IA seeks for the intersection between two sets whenever possible. Otherwise, the algorithm will find out the minimum distance between

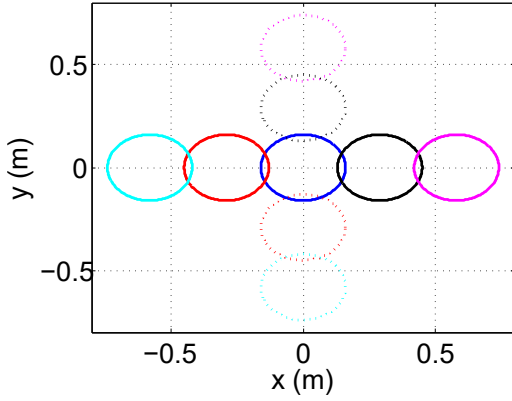


Fig. 3: Near-field specifications for the multi-spot coverage area.

both. First set ( $\mathcal{M}$ ) is defined wherein all the fields that fulfill the specifications, then, the other set ( $\mathcal{R}$ ) gathers all the fields which can be radiated by the antenna, regarding the optics [7]. The projection from one set to the other is performed by alternative projection thus, two projectors need to be defined. The forward projector ( $\mathcal{F}$ ) performs the projection from  $\mathcal{R}$  to  $\mathcal{M}$ , and the backward projection ( $\mathcal{B}$ ) that projects a point from ( $\mathcal{M}$ ) onto ( $\mathcal{R}$ ). The IA iteratively uses both projectors in each iteration as follow:

$$\vec{E}_{i+1} = \mathcal{B} \left[ \mathcal{F} \left( \vec{E}_i \right) \right] \quad (1)$$

where  $\vec{E}$  is the radiated field and  $i$  the current iteration.

Before applying the forward projection, it is necessary to define the bounds within the near-field satisfy the requirements. These limits are given in terms of templates, regarding that one of them is for the lower bound and other for the upper one. In addition, these templates have to be extended for the whole volume where the near-field is computed. Then, after the near-field computation, the forward projection trims the field according the  $P_{\mathcal{F}}$  operator, which is defined as follow:

$$P_{\mathcal{F}}^2 \left( |F|^2 \right) = \begin{cases} T_{\max}(x, y)^2 & \text{if } |F(x, y)|^2 \geq T_{\max}(x, y)^2 \\ |F(x, y)|^2 & \text{if } T_{\min}(x, y)^2 \leq |F(x, y)|^2 \leq T_{\max}(x, y)^2 \\ T_{\min}(x, y)^2 & \text{if } |F(x, y)|^2 \leq T_{\min}(x, y)^2 \end{cases} \quad (2)$$

where  $T_{\min}(x, y)$  and  $T_{\max}(x, y)$  are the lower and upper bound templates respectively and  $F(x, y)$  is the magnitude of the near-field radiated by the antenna.

On the other hand, if the synthesis is done over the near-field, the backward projection has a drawback regarding the far-field case. While in far-field optimization the FFT is used as the backward projection [8], achieving a very efficient algorithm, in near-field synthesis the FFT is not available since it cannot be used in the computation of the near-field. Thus, a new definition of this projector is required. Accordingly, the distance definition in the Euclidean space  $L^2$  can be apply on

the distance from an element belonging to the set  $\mathcal{M}$  to  $\mathcal{R}$ . Therefore, this distance can be expressed as:

$$d = \iint_{\Omega} C(x, y) \cdot \left( |F'(x, y)|^2 - |F(x, y)|^2 \right)^2 dx dy \quad (3)$$

where  $F(x, y)$  is the magnitude of the near-field radiated by the antenna;  $F'(x, y)$  is the magnitude of the near-field within the boundaries since the  $P_{\mathcal{F}}^2$  was applied;  $\Omega$  is the surface where the near-field is calculated and  $C(x, y)$  is a weighting function.

If the volume where the near-field is computed is sampled in different parallel planes, the radiated field is discretized in a  $XY$  grid, changing (3) as:

$$d = \sum_z \sum_{xy} \left[ C(x, y) \cdot \left( |F'(x, y)|^2 - |F(x, y)|^2 \right)^2 \Delta x \Delta y \right] \quad (4)$$

where  $F(x, y)$  is the magnitude of the near-field in a  $XY$  plane;  $F'(x, y)$  is the magnitude of the trimmed near-field in a  $XY$  plane and  $C(x, y)$  is a weighting function.

This new expression can be minimize using a general algorithm, such as the Levenberg-Marquardt Algorithm (LMA) [9]. Thus, the minimization of (4) leads to either the intersection or the minimum distance between both sets.

## IV. RESULTS

### A. Transmitarray definition

Taking the centre of the transmitarray as the origin of the coordinates system and, the central feed at  $(\hat{x}, \hat{y}, \hat{z}) = (0, 0, -0.100)$  m, the position of the other feeds can be easily computed as  $(r \sin \beta, 0, r \cos \beta)$  for the  $xz$  cut and  $(0, r \sin \alpha, r \cos \alpha)$  for the  $yz$  cut, where  $r$  is the  $\hat{z}$  position of the central feed ( $-0.100$  m). Applying these equations with  $\beta = \alpha = 10^\circ$ , the location of the feeds are computed and the results are shown in Table IV-A.

TABLE I: Position of the feeds.

Feeder	#0	#(1 3)	#(2 4)	#(5 7)	#(6 8)
$\hat{x}$	0	$\pm 0.0174$	$\pm 0.0342$	0	0
$\hat{y}$	0	0	0	$\pm 0.0174$	$\pm 0.0342$
$\hat{z}$	0.100	0.0985	0.0940	0.0985	0.0940

Then, a transmitarray of 576 elements in a  $24 \times 24$  regular grid has been chosen. Both  $\hat{x}$  and  $\hat{y}$  periodicity is  $5 \times 5 \text{mm}^2$  so, the equivalent aperture ( $D$ ) is  $120 \times 120 \text{mm}^2$  or  $11.2\lambda \times 11.2\lambda$  at a central frequency of 28 GHz. The feeds of the cluster are modeled as an ideal horn with a  $\cos^q \theta$  function and a  $q$ -factor of 20. Regarding these parameters the incident field over the transmitarray surface is computed, in order to analyse the similarity between the central feed and the extreme ones, which is the worst case. In these conditions, the incident fields obtained are depicted in Fig. 4, showing that both field are similar and only slight differences can be found, mainly because of the different projection of the incident field on the transmitarray surface for each feed.

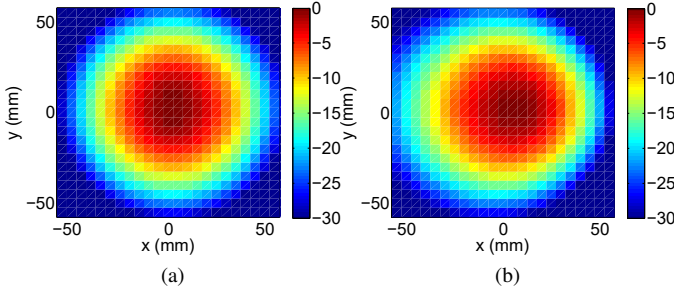


Fig. 4: Incident field of the (a) central feed (# 0) (b) feed # 4.

### B. Far-field focussed transmitarray

In a first approach, a far-field focussed transmitarray is considered, whereby the radiated field is a pencil beam in a certain  $\theta_0$  direction. In addition, the phase distribution of this kind of antennas can be easily computed as:

$$\phi_t(x_m, y_n) = \phi_{inc}(x_m, y_n) - k_0 x_i \sin \theta_0 \quad (5)$$

where  $\phi_{inc}(x_m, y_n)$  is the phase of the incident field at the  $(m, n)$ -th element;  $k_0$  is the vacuum wavenumber and  $\theta_0$  is the pointing direction. This equation provide the phase of the transmission coefficient for the  $X$  (see Fig. 5) or  $Y$  polarization. Although the transmitarray is feed by a cluster, the desing is done by a single feed, in this case, the central one. Thus, taking Fig. 2 as reference, the central beam is radiated in the direction  $\hat{z}_a$  and  $\theta_0$  equal to  $0^\circ$ . Then, the position of the other feeds are outlined at Tab.I, which are computed with the equations defined previously.

The near-field coverage area obtained with this approach by the cluster is shown in Fig. 6, where the field is normalized by its maximum and the curves represent the  $-1$  and  $-3$  dB level. According with the figure, this transmitarray does not allow to obtain a continuous and flat coverage with maximum ripple of 1 dB. Thus, a synthesis process is required to improve the performance of the antenna. The goal of the synthesis will be to ensure a ripple lower than 1 dB for the coverage of the zones defined by the green circunferences in the figure.

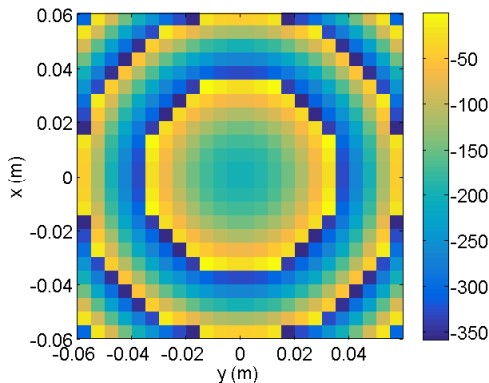


Fig. 5: Initial phase distribution obtained using (5).

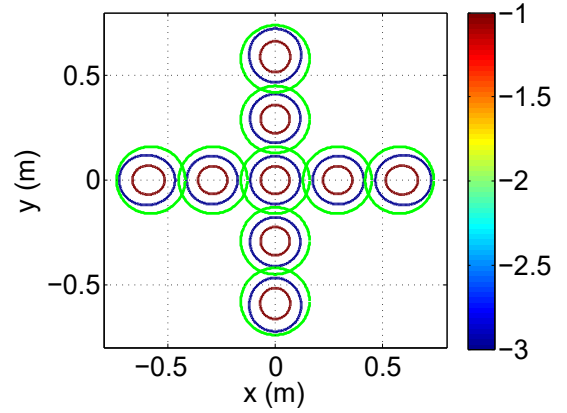


Fig. 6: Initial near-field coverage area radiated by the phase initial phase distribution normalized by each maximum (red line)  $-1$ dB (blue line)  $-3$ dB level. (green line) optimization coverage area for 1 dB amplitude ripple

### C. Results for the optimized transmitarray

The synthesis process is carried out only for the central feed and the improvement produced for the different spots is evaluated then. After 1200 iterations the algorithm reached a solution that fulfill the previous requirements for the central spot. The resulting phase distribution is shown in Fig. 7.

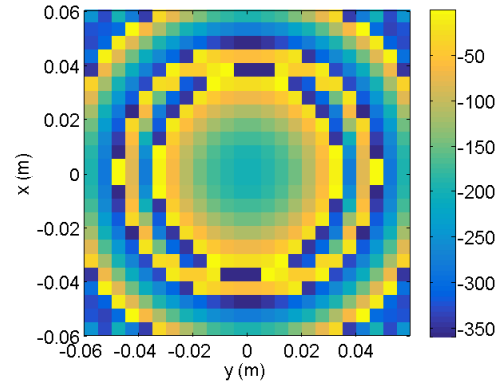


Fig. 7: Phase distribution obtained as result of the optimization process.

The near-field coverage area generated by the phase distribution after the optimization process is shown in Fig. 8, where it is possible to verify that generally the size of the coverage area has increased and consequently the performances of the antenna. Particularly, the central spot totally satisfies a ripple lower than 1 dB within the green line, regarding that this spot was the only one that was optimized. Then, the adjacent beams have also increased its size, although the specification is not totally fulfilled, it is close to reach less than 1 dB of magnitude ripple within the desire area. Another aspect that can be outlined in these four adjacent beams is a slight shift of the beam, accordingly to this fact the beam losses its simmetry and it is harder to keep the beam within the green

lines. This effect is mostly significant in the external beams, which have suffered a bigger shift and have entirely lost its symmetry. All of these effects can be also observed in Fig. 9, where the cut  $y = 0$  is shown for the starting and optimized point. Nevertheless, it is highlighted that although the beam is shifted the size of the  $-1$  dB is increased and really closed to the initial specifications and can be corrected by the suitable modification of the feeds.

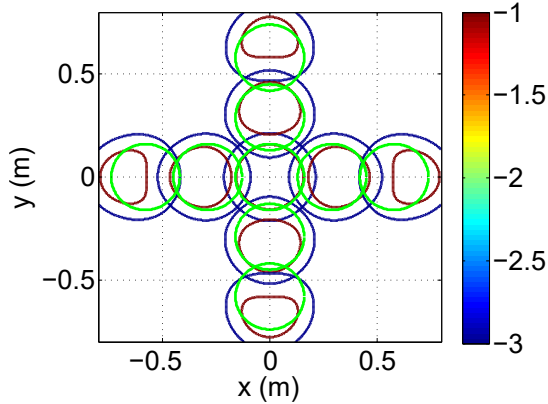


Fig. 8: Near-field coverage area after the optimization normalized by each maximum (red line)  $-1$ dB (blue line)  $-3$ dB level. (green line) optimization coverage area for 1 dB amplitude ripple

## V. CONCLUSION

A transmitarray antenna is proposed to be used as a base station at 28 GHz for giving indoor coverage areas, in particular, femtocells or near-field coverage areas. The transmitarray is fed by a spatially distributed array, which helps to improve the features of the base station in terms of capacity. This setup provides different spots that can be used for giving coverage but there are two main drawbacks that limit the size of each area. First, the transmitarray is designed taking only one feed into account and then, the taper of the incident field is reproduced in the reflected field, therefore, the size of the spot is also affected. Both issues are reduced applying an optimization using the Intersection Approach Algorithm. Although in the optimization process only one feed is considered, the results show an improvement for the whole cluster. Finally, in the light of the results it is feasible to establish that working using only one feed in the optimization and then placing the others at certain locations can improve the results without the need of carrying out a multi-position optimization.

## REFERENCES

- [1] J. Huang, C. Wang, R. Feng, J. Sun, W. Zhang and Y. Yang, "Multi-Frequency mmWave Massive MIMO Channel Measurements and Characterization for 5G Wireless Communication Systems," *IEEE Journal on Selected Areas in Communications*, vol. 35, pp. 1591–1605, April 2017.
- [2] E.L. Bengtsson, F. Rusek, S. Malkowsky, F. Tufvesson, P.C. Karlsson, and O. Edfors, "A Simulation Framework for Multiple-Antenna Terminals in 5G Massive MIMO Systems," *IEEE Journal on Selected Areas in Communications*, vol. 35, pp. 1591–1605, April 2017.

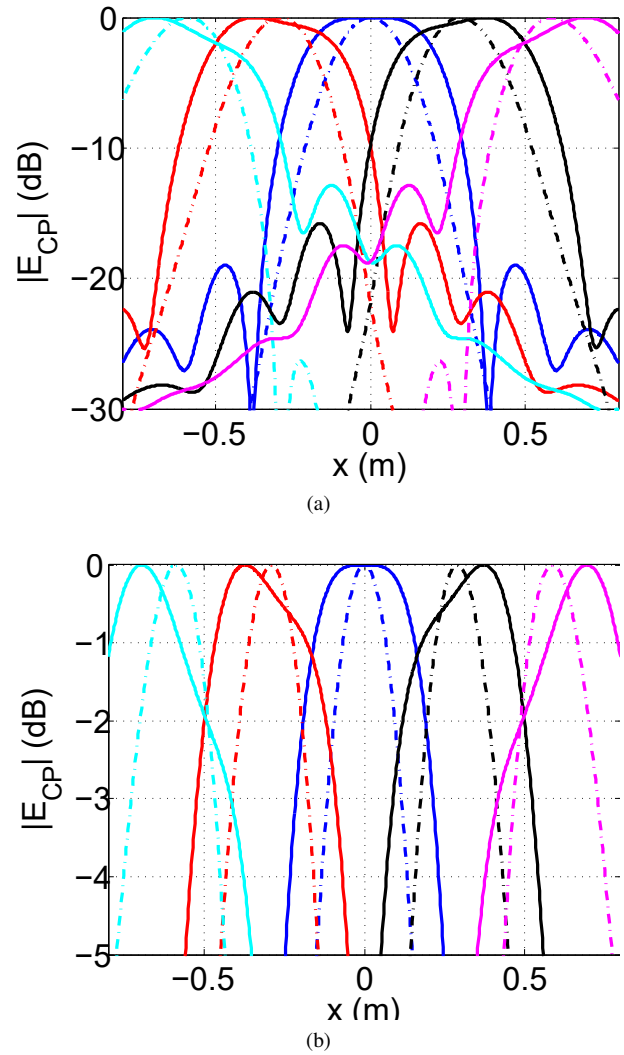


Fig. 9: (a) Cut at  $y = 0$  for the normalized near-field (dashed line) before and (solid line) after the optimization process (b) zoom of (a).

- [3] C.A. Fernandes, and L.M. Anunciada, "Constant flux illumination of square cells for millimeter-wave wireless communications," *IEEE Transactions on Microwave Theory and Techniques*, vol. 49, pp. 2137–2141, November 2001.
- [4] D.R. Prado, and M. Arrebola, "Effective XPD and XPI Optimization in Reflectarrays for Satellite Missions," *IEEE Antennas and Wireless Propagation Letters*, vol. 17, pp. 1856–1860, September 2018.
- [5] J.A. Encinar, R. Florencio, M. Arrebola, M.A. Salas, M. Barba, R.R. Boix, and G. Toso, "Dual-polarization reflectarray in Ku-band based on two layers of dipole-arrays for a transmit-receive satellite antenna with South American coverage," *11th European Conference on Antennas and Propagation (EuCAP)*, Paris (France), March 2017.
- [6] A.F. Vaquero, D.R. Prado, M. Arrebola, and M.R. Pino, "Reflectarray Antennas for 5-G Indoor Coverage," *13th European Conference on Antennas and Propagation (EuCAP)*, Krakow (Poland), April 2019.
- [7] O.M. Bucci, G.D. Elia, G. Mazzarella and G. Panariello, "Antenna pattern synthesis: a new general approach," *Proc. IEEE*, vol. 82, pp. 358–371, March 1994.
- [8] J.A. Zornoza, and J.A. Encinar, "Efficient phase-only synthesis of contoured-beam patterns for very large reflectarrays," *Int. J. RF Microw. Comput. Eng.*, vol.14, pp. 415–423, September 2004.
- [9] D.R. Prado, J.Álvarez, M. Arrebola, M.R. Pino, R.G. Ayestarán, and F. Las-Heras, "Efficient, accurate and scalable reflectarray phase-only

synthesis based on the Levenberg-Marquardt algorithm,” Appl. Comp. Electro. Society (ACES) Journal, vol.30, pp. 1246-1255, December 2015.